Article



# Interaction of S100A6 Protein with the Four-Helical Cytokines

Alexey S. Kazakov , Evgenia I. Deryusheva , Victoria A. Rastrygina , Andrey S. Sokolov , Maria E. Permyakova , Ekaterina A. Litus , Vladimir N. Uversky * , Eugene A. Permyakov , Sergei E. Permyakov *

Posted Date: 28 July 2023

doi: 10.20944/preprints202307.2030.v1

Keywords: cytokine; EF-hand; S100 protein; S100A6; protein–protein interaction

*Article*

# Interaction of S100A6 Protein with the Four-Helical Cytokines

**Alexey S. Kazakov [1], Evgenia I. Deryusheva [1], Victoria A. Rastrygina [1], Andrey S. Sokolov [1], Maria E. Permyakova [1], Ekaterina A. Litus [1], Vladimir N. Uversky [1,2,*], Eugene A. Permyakov [1] and Sergei E. Permyakov [1,*]**

[1] Institute for Biological Instrumentation, Pushchino Scientific Center for Biological Research of the Russian Academy of Sciences, Institutskaya str., 7, Pushchino, Moscow Region 142290, Russia; fenixfly@yandex.ru (A.S.K.); janed1986@ya.ru (E.I.D.); certusfides@gmail.com (V.A.R.); 212sok@gmail.com (A.S.S.); mperm1977@gmail.com (M.E.P.); ealitus@gmail.com (E.A.L.); epermyak@yandex.ru (E.A.P.)

[2] Department of Molecular Medicine and USF Health Byrd Alzheimer's Research Institute, Morsani College of Medicine, University of South Florida, Tampa, FL 33612, USA; vuversky@usf.edu

* Correspondence: vuversky@usf.edu (V.N.U.); permyakov.s@gmail.com (S.E.P.); Tel.: +7-(495)-143-7740 (S.E.P.); Fax: +7-(4967)-33-05-22 (S.E.P.)

**Abstract:** S100 is a family of over 20 structurally homologous, but functionally diverse regulatory (calcium/zinc)-binding proteins of vertebrates. The involvement of S100 proteins in numerous vital (patho)physiological processes is mediated by their interaction with various (intra/extra)cellular protein partners, including cell surface receptors. Furthermore, recent studies revealed the ability of specific S100 proteins to affect cell signaling via direct interaction with cytokines. Previously, we have revealed binding of ca. 71% of the four-helical cytokines by S100P protein due to the presence in its molecule of a cytokine-binding site, which overlaps with the binding site for S100P receptor. Here we show that another S100 protein, S100A6 (pairwise sequence identity with S100P of 35%), specifically binds numerous four-helical cytokines. We have studied affinity of recombinant forms of 35 human four-helical cytokines covering all structural families of this fold to Ca2+-loaded recombinant human S100A6, using surface plasmon resonance spectroscopy. S100A6 recognizes 26 of the cytokines from all families of this fold with the equilibrium dissociation constants ranging from 0.3 nM to 12 μM. Overall, S100A6 interacts with ca. 73% of the four-helical cytokines studied to date with selectivity equivalent to that for S100P protein, with the differences limited to binding of Interleukin-2 and Oncostatin-M. The molecular docking study evidences presence in S100A6 molecule of a cytokine-binding site, analogous to that found in S100P. The findings argue the presence in some of the promiscuous members of S100 family of a site specific to a wide range of the four-helical cytokines. This unique feature of the S100 proteins potentially allows them to serve as universal inhibitors of signaling of the four-helical cytokines, which could be of value for reduction of severity of the disorders accompanied by excessive release of the cytokines.

**Keywords:** cytokine; EF-hand; S100 protein; S100A6; protein–protein interaction

## 1. Introduction

S100 is an evolutionary young family of structurally similar, but functionally diversified regulatory $Ca^{2+}$-binding proteins of the EF-hand superfamily (for reviews, see [1–4]). The canonical $Ca^{2+}$-binding motif of 'EF-hand' type (PROSITE [5] entry PDOC00018) is composed of a 12-residue $Ca^{2+}$-coordinating loop flanked by two $\alpha$-helices [6,7]. S100 proteins consist of a low-affinity non-classical N-terminal EF-hand motif and a high-affinity classical C-terminal EF-hand, which are connected by a flexible 'hinge' region [7,8]. Certain S100 proteins possess distinct $Zn^{2+}$/$Cu^{2+}$/$Mn^{2+}$-binding sites [8,9]. S100 proteins are generally considered to be (homo/hetero)dimeric (except for monomeric S100G), whereas some of them tend to form higher order oligomers [2,10]. With the exception of the S100 fused-type proteins, human S100 family includes 21 members (78-113 residues;

 doi:10.20944/preprints202307.2030.v1



pairwise sequence identity calculated using Clustal Omega 2.1 [11] ranges from 16% to 61%), each of which has a unique set of functional activities, overall covering nearly all vital processes [1–3]. Some S100 proteins are associated with progression of oncological, inflammatory, autoimmune, neurodegenerative, cardiovascular, and pulmonary diseases, are used for diagnostic and prognostic purposes, and are considered as promising therapeutic targets [12–18]. The dysregulated expression of most S100 proteins in cancer is related to the fact that they are mainly encoded by the epidermal differentiation complex located on human chromosome 1 (locus 1q21), which is frequently rearranged in cancer [19,20]. The S100 genes located on chromosome 1 and their protein products are designated by Arabic numbers placed behind the 'S100A' (*e.g.*, S100A1), while S100 genes originating from other chromosomes carry the stem symbols 'S100' followed by a single letter (*e.g.*, S100P) [20,21]. The multifunctionality of S100 proteins is due to their tissue/cell-specific expression, ability to localize in the cytosol/nucleus/extracellular space, metal-binding properties, post-translational modifications, and propensity to recognize a wide range of targets, including enzymes, transcription factors, receptor/membrane proteins, lipids, and nucleic acids [1–3,22].

Despite the lack of a leader sequence, some of S100 proteins are secreted in a cell-dependent manner via the classical endoplasmic reticulum (ER)/Golgi pathway or several unconventional passive and active mechanisms [2,23,24]. When released into the extracellular space, certain S100 proteins exert a cytokine-like action due to interaction with specific cell surface receptors, such as RAGE, TLR4, ErbB1, ErbB3, ErbB4, IL-10R, integrin β1, neuroplastin-β, 5-$HT_{1B}$, 4-$HT_4$, SIRL-1, ALCAM, EMMPRIN, CD33, CD36, CD68, CD69, CD146 [2,22,25–32]. Moreover, some of the released S100 proteins interact with cytokines. For instance, S100A4 binds ErbB1/ErbB4 ligands [31,33], S100A13 interacts with IL1α/FGF1 [34,35], S100B binds FGF2 [36], S100A11/A12/A13 interact with soluble form of TNF [37]. Several S100 proteins recognize four-helical cytokines: S100A2/A6/P bind EPO [38], S100A1/A4/A6/B/P interact with IFN-β [22,39,40], distinct subsets of S100A1/A6/B/P bind to specific IL-6 family cytokines (IL-11, OSM, CNTF, CT-1, and CLCF1 [41]), whereas S100P binds 29 four-helical cytokines [42]. The S100 binding has been shown to affect the cytokine signaling in some cases: S100A4 enhanced the amphiregulin-mediated proliferation of embryonic fibroblasts [33], S100B inhibited FGF2-induced increase in proliferation of MCF-7 and MDA-MB468 cells [36], S100A12/A13 rescued Huh-7 cells from the cytotoxic effect of soluble TNF [37], and S100A1/A4/B/P proteins suppressed the IFN-β-induced inhibition of viability of MCF-7 cells [22,39,40]. Besides, S100-cytokine interactions can promote non-classical secretion of the cytokines as exemplified by S100A13 - IL1α/FGF1 interactions [34,35].

The vast majority of the established S100-cytokine interactions correspond to cytokines belonging to the superfamily of four-helical cytokines (SCOP [43] ID: 3001717), which is subdivided into three families: 'Short-chain cytokines' (SCOP ID 4000852), 'Long-chain cytokines' (SCOP ID 4000851) and 'Interferons/interleukin-10 (IL-10)' (SCOP ID 4000854). We have previously shown that S100P oncoprotein is poorly selective towards the four-helical cytokines of all structural families, interacting with 71% of them (29 out of the 41 cytokines studied) with the equilibrium dissociation constants, $K_d$, in the range from 1 nM to 3 μM (below the $K_d$ value for S100P complex with V domain of RAGE) [42]. Using mutagenesis, we confirmed the presence of a cytokine-binding site in S100P molecule, overlapping with its RAGE-specific site. The ability of S100P to recognize multiple cytokines reflects its promiscuous nature, well established for certain members of S100 family, which readily share their binding partners [44,45]. Therefore, the specificity to many four-helical cytokines is also expected for other promiscuous representatives of S100 family. To explore this possibility, in this work we test the affinity of another promiscuous S100 oncoprotein [44,45], S100A6 (also known as calcyclin; pairwise sequence identity to S100P of 35%), specific to 6 four-helical cytokines shown in Table 1, to a panel of 35 four-helical cytokines from all their structural families (Table 2). Our findings greatly expand the long list of known extracellular target proteins of S100A6, which may be of value for deciphering its role in progression of many cancers (positive correlation between S100A6 expression and the disease stage, tumor size and/or metastasis is reported), myocardial infraction, acute coronary syndrome, chronic renal disease, primary biliary cholangitis, pulmonary fibrosis,

Preprints (www.preprints.org) | NOT PEER-REVIEWED | Posted: 28 July 2023 doi:10.20944/preprints202307.2030.v1



systemic sclerosis of the lung, endometriosis, various eye pathologies, and other disorders (reviewed in [46]).

**Table 1.** The literature data on equilibrium dissociation constants for the complexes between $Ca^{2+}$-loaded S100A6 and four-helical cytokines at 25ºC. The SPR spectroscopy data (amine coupling of the cytokine on the SPR chip surface) are described using the *heterogeneous ligand* model (1).

| Cytokine | $K_{d1}$, M | $K_{d2}$, M | Reference |
|---|---|---|---|
| Short-chain cytokines | | | |
| EPO | $(1.5 \pm 0.3) \times 10^{-7}$ | $(6.5 \pm 2.6) \times 10^{-7}$ | [38] |
| Long-chain cytokines | | | |
| CLCF1 | $(1.1 \pm 0.8) \times 10^{-6}$ | $(3.7 \pm 0.8) \times 10^{-6}$ | [41] |
| CNTF | $(1.1 \pm 1.0) \times 10^{-7}$ | $(2.07 \pm 0.08) \times 10^{-6}$ | [41] |
| CT-1 | $(1.6 \pm 0.5) \times 10^{-6}$ | $(1.2 \pm 0.4) \times 10^{-5}$ | [41] |
| IL-11 | $(8.3 \pm 1.9) \times 10^{-6}$ | $(7.9 \pm 2.1) \times 10^{-6}$ | [41] |
| Interferons/IL-10 | | | |
| IFN-β | $(8.2 \pm 2.4) \times 10^{-8}$<br>$(0.70 \pm 0.03) \times 10^{-9}$ * | $(2.67 \pm 0.57) \times 10^{-7}$<br>$(2.81 \pm 0.49) \times 10^{-7}$ * | [39] |

* S100A6 serves as a ligand

**Table 2**. The cytokine samples studied with regard to affinity to $Ca^{2+}$-loaded S100A6 in the present work.

| Full name | Abbreviation | UniProt ID | Manufacturer | Cat. number | Source |
|---|---|---|---|---|---|
| Short-chain cytokines | | | | | |
| Fms-related tyrosine kinase 3 ligand | Flt3L | P49771 | PeproTech | 300-19 | *E.coli* |
| Granulocyte-macrophage colony-stimulating factor | GM-CSF | P04141 | PeproTech | 300-03 | *E.coli* |
| Interleukin-2 | IL-2 | P60568 | PeproTech | AF-200-02 | *E.coli* |
| Interleukin-3 | IL-3 | P08700 | SCI-Store (Russia) | PSG160-10 | CHO |
| Interleukin-4 | IL-4 | P05112 | PeproTech | AF-200-04 | *E.coli* |
| Interleukin-5 | IL-5 | P05113 | PeproTech | 200-05 | *E.coli* |
| Interleukin-7 | IL-7 | P13232 | SCI-Store (Russia) | PSG240-10 | CHO |
| Interleukin-9 | IL-9 | P15248 | PeproTech | 200-09 | *E.coli* |
| Interleukin-13 | IL-13 | P35225 | PeproTech | 200-13 | *E.coli* |
| Interleukin-15 | IL-15 | P40933 | PeproTech | 200-15 | *E.coli* |
| Interleukin-21 | IL-21 | Q9HBE4 | PeproTech | 200-21 | *E.coli* |
| Macrophage colony-stimulating factor 1 | M-CSF | P09603 | PeproTech | 300-25 | *E.coli* |
| Stem cell factor, soluble form | SCF | P21583 | PeproTech | 300-07 | *E.coli* |
| Thrombopoietin | THPO | P40225 | SCI-Store (Russia) | PSG090-10 | CHO |
| Thymic stromal lymphopoietin | TSLP | Q969D9 | PeproTech | 300-62 | *E.coli* |
| Long-chain cytokines | | | | | |
| Chorionic somatomammotropin hormone 1 | PL | P0DML2 | R&D Systems | 5757-PL/CF | CHO |
| Granulocyte colony-stimulating factor | G-CSF | P09919 | Pharmstandard (Russia) | n/a | *E.coli* |

 doi:10.20944/preprints202307.2030.v1



| | | | | | |
|---|---|---|---|---|---|
| Growth hormone | GH | P01241 | PeproTech | AF-100-40 | *E.coli* |
| Growth hormone variant | GH-V | P01242 | R&D Systems | 7668-GH/CF | *E.coli* |
| Interleukin-12 | IL-12 | P29459* & P29460 | PeproTech | 200-12H | HEK293 |
| Interleukin-23 | IL-23 | Q9NPF7* & P29460 | PeproTech | 200-23 | Hi-5 |
| Interleukin-27 | IL-27 | Q8NEV9* & Q14213 | PeproTech | 200-38 | HEK293 |
| Interleukin-31 | IL-31 | Q6EBC2 | PeproTech | 200-31 | E.coli |
| Interleukin-35 | IL-35 | P29459* & Q14213 | PeproTech | 200-37 | HEK293 |
| Leptin | LEP | P41159 | PeproTech | AF-300-27 | E.coli |
| Prolactin | PRL | P01236 | PeproTech | 100-07 | E.coli |
| Interferons/IL-10 | | | | | |
| Interferon α-2 | IFN-α2 | P01563 | Vector-Medica (Russia) | n/a | E.coli |
| Interferon γ | IFN-γ | P01579 | Pharmaclon (Russia) | n/a | E.coli |
| Interferon ω-1 | IFN-ω1 | P05000 | PeproTech | 300-02J | E.coli |
| Interleukin-10 | IL-10 | P22301 | PeproTech | AF-200-10 | E.coli |
| Interleukin-19 | IL-19 | Q9UHD0 | PeproTech | 200-19 | E.coli |
| Interleukin-20 | IL-20 | Q9NYY1 | PeproTech | 200-20 | E.coli |
| Interleukin-22 | IL-22 | Q9GZX6 | PeproTech | 200-22 | E.coli |
| Interleukin-24 | IL-24 | Q13007 | PeproTech | 200-35 | CHO |
| Interleukin-26 | IL-26 | Q9NPH9 | R&D Systems | 1375-IL/CF | E.coli |

* denotes the chain used for SCOP 2 [43] family assignment. n/a, not applicable

## 2. Materials and methods

### *2.1. Materials*

Human S100A6 protein was prepared in *E. coli* as described in [39]. The samples of human cytokines are presented in Table 2. Protein concentrations were measured spectrophotometrically according to [47].

Sodium acetate and ethanolamine were from Bio-Rad Laboratories, Inc. HEPES and sodium chloride were purchased from PanReac AppliChem. $CaCl_2$, EDTA and TWEEN 20 were from Sigma Aldrich Co.

### *2.2. Surface plasmon resonance studies*

SPR studies of S100A6 binding to the cytokines immobilized on the sensor chip surface (S100A6 was used as an analyte and the cytokines served as ligands) were performed at 25°C mainly as described in [42]. Cytokine (0.03-0.05 mg/ml) in 10 mM sodium acetate pH 4.5 buffer was immobilized on ProteOn™ GLH sensor chip surface of ProteOn™ XPR36 instrument (Bio-Rad Laboratories, Inc.) by amine coupling (up to 10 000 - 17 000 RUs). The remaining activated amine groups on the chip surface were blocked with 1 M ethanolamine solution. S100A6 (63 nM - 8 μM) solution in the running buffer (10 mM HEPES, 150 mM NaCl, 1 mM $CaCl_2$, 0.05% TWEEN 20, pH 7.4) was passed over the chip surface at a rate of 30 μl/min for 300 s, followed by passage of the running buffer for 1 200 – 2 400 s. The double-referenced SPR sensograms were described by either a single

Preprints (www.preprints.org) | NOT PEER-REVIEWED | Posted: 28 July 2023 doi:10.20944/preprints202307.2030.v1



site binding model (S100A6 - IL-2 interaction) or a *heterogeneous ligand* model (1). The latter suggests existence of two populations of the ligand ($L_1$ and $L_2$) that bind a single analyte molecule (A):

$$L_1 + A \underset{k_{d1}}{\overset{k_{a1}}{\rightleftarrows}} L_1A \qquad L_2 + A \underset{k_{d2}}{\overset{k_{a2}}{\rightleftarrows}} L_2A \qquad (1)$$

$$K_{d1} \qquad K_{d2}$$

Here, $k_a$ and $k_d$ are kinetic association and dissociation constants, respectively; $K_d$ are equilibrium dissociation constants ($k_d/k_a$). The $K_d$ and $k_d$ values were evaluated for each S100A6 concentration using ProteOn Manager™ v.3.1 software (Bio-Rad Laboratories, Inc.). The resulting values are average of 3-5 estimates (the standard deviations are indicated). The ligand was regenerated by 20 mM EDTA solution pH 8.0 for 100 s. The free energy changes, accompanying the reaction were calculated as follows: $\Delta G_i = - RT \ln(55.3/K_{di})$, i=1,2.

### *2.3. Structural classification of cytokines*

The cytokines investigated in this study were classified according to the SCOP 2 database (https://scop2.mrc-lmb.cam.ac.uk [43], build 1.0.6, updated on 06-29-2022) as belonging to the 'All alpha proteins' structural class, '4-helical cytokines' fold (SCOP ID 2001054), '4-helical cytokines' superfamily (SCOP ID 3001717). This superfamily comprises three families, namely 'Short-chain cytokines' (SCOP ID 4000852), 'Long-chain cytokines' (SCOP ID 4000851) and 'Interferons/interleukin-10 (IL-10)' (SCOP ID 4000854). CLCF1 and CT-1 were classified as the long-chain cytokines according to [48].

### *2.4. Structural modeling of the S100A6-cytokine complexes*

The ClusPro docking server [49] was used to generate the models of tertiary structures of the S100A6-cytokine complexes, as previously described [38,42]. The structure of the $Ca^{2+}$-loaded human S100A6 dimer was taken from PDB [50] entry 1K9K (X-ray, chains A and B [51]), while the tertiary structures of the four-helical cytokines were either extracted from PDB (including the complexes with their binding partners) or predicted using AlphaFold2 (https://alphafold.ebi.ac.uk/ [52]) (Table S1). Ten docking models were taken into account for each S100A6-cytokine pair. The contact residues included into five or more docking models were considered as the most probable residues of the binding site. Distributions of the predicted contact residues of S100A6 over its amino acid sequence within the models of S100A6 complexes with specific cytokines were calculated as described in [38]. The tertiary structures were visualized using the molecular graphics system PyMOL v.2.5.0 (https://pymol.org/2/).

## 3. Results and discussion

### *3.1. Selectivity of S100A6 binding to the four-helical cytokines*

We have studied affinity of $Ca^{2+}$-loaded (1 mM $CaCl_2$) recombinant human S100A6 protein to the panel of 35 recombinant human four-helical cytokines (includes the panel used in [42], extended by Flt3L, SCF and IL-19), which covers all structural families of this fold (Table 2). The cytokines were immobilized on the surface of SPR sensor chip by amine coupling, and 61 nM - 8 μM solutions of S100A6 were passed over the surface at 25ºC. Whereas 9 cytokines (Table S2) did not reveal noticeable effects in response to the S100A6 (data not shown), the SPR sensograms for 26 cytokines showed the S100A6 concentration-dependent effects, characteristic of the association-dissociation processes (Figures 1–4). The kinetic SPR data were adequately described within the heterogeneous ligand model (1) (Figures 1–4, Table 3), which was earlier successfully used for description of the S100-cytokine interactions [22,38–42,53,54]. The data for IL-2 were described by the one-site binding scheme. The respective equilibrium dissociation constants, $K_d$, range from 0.3 nM (in the case of THPO, similarly to S100P [42]) to 12 μM (for IL-2) (Table 3). For comparison, the reported SPR estimates of $K_d$ values for the complexes of Ca2+-bound S100A6 with various extracellular fragments

Preprints (www.preprints.org) | NOT PEER-REVIEWED | Posted: 28 July 2023 doi:10.20944/preprints202307.2030.v1



of its receptor, RAGE, are within the range from 28 nM to 13 μM [55,56], whereas the $K_d$ value for V domain of RAGE measured by isothermal calorimetry is of 3 μM [57]. An analysis of the free energy changes upon the S100A6-cytokine interactions (Figure 5), ΔG, shows that the average S100A6 affinities for the cytokines of different SCOP families of the fold decrease in the following order: short-chain cytokines > long-chain cytokines > interferons/IL-10 (ΔG of -49.8 kJ/mol < -47.1 kJ/mol < -46.8 kJ/mol). The same tendency was observed previously for S100P protein [42].

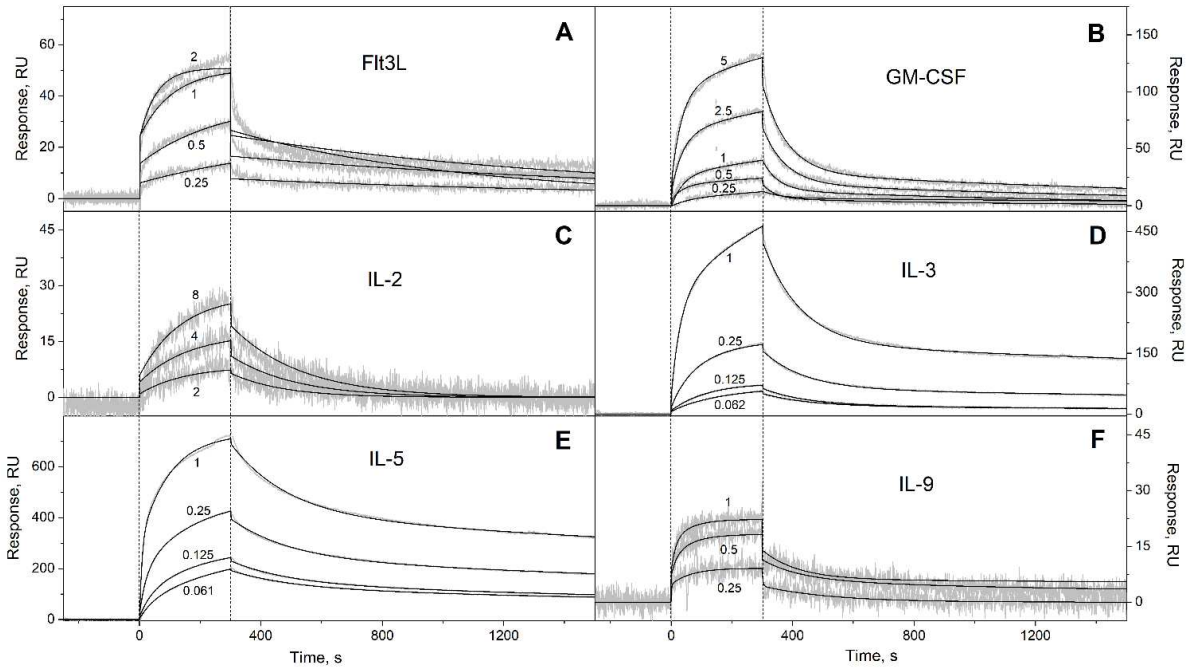


**Figure 1.** SPR spectroscopy data on kinetics of association/dissociation of the complexes of $Ca^{2+}$-bound S100A6 with the short-chain four-helical cytokines (see Table 3) immobilized on the sensor chip surface by amine coupling, 25°C (10 mM HEPES, 150 mM NaCl, 1 mM $CaCl_2$, 0.05% TWEEN 20, pH 7.4). The association phase is marked by the vertical dotted lines. Micromolar concentrations of S100A6 are indicated for the sensograms. The experimental curves (*grey*) are described by the *heterogeneous ligand* model (1) or one-site binding model (*black curves*) (see Table 3).

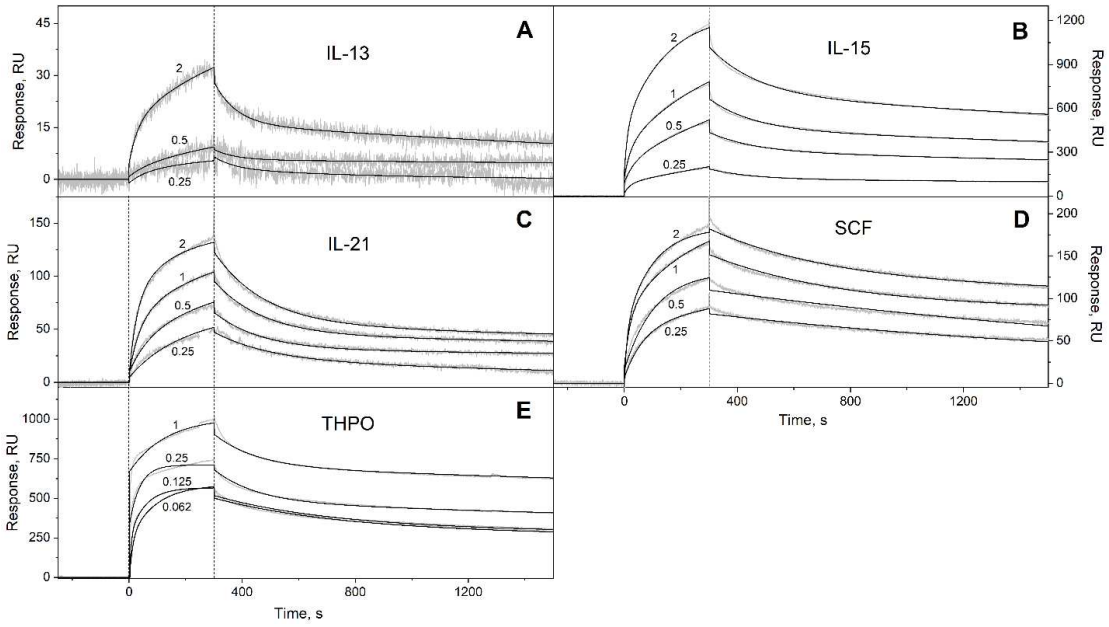


**Figure 2.** SPR spectroscopy data on kinetics of association/dissociation of the complexes of $Ca^{2+}$-bound S100A6 with the short-chain four-helical cytokines (see Table 3) immobilized on the sensor chip

Preprints (www.preprints.org) | NOT PEER-REVIEWED | Posted: 28 July 2023 doi:10.20944/preprints202307.2030.v1



surface by amine coupling, 25°C (10 mM HEPES, 150 mM NaCl, 1 mM $CaCl_2$, 0.05% TWEEN 20, pH 7.4). The experimental curves (*grey*) are described by the *heterogeneous ligand* model (1) (*black curves*) (see Table 3). For other designations, refer to the caption to Figure 1.

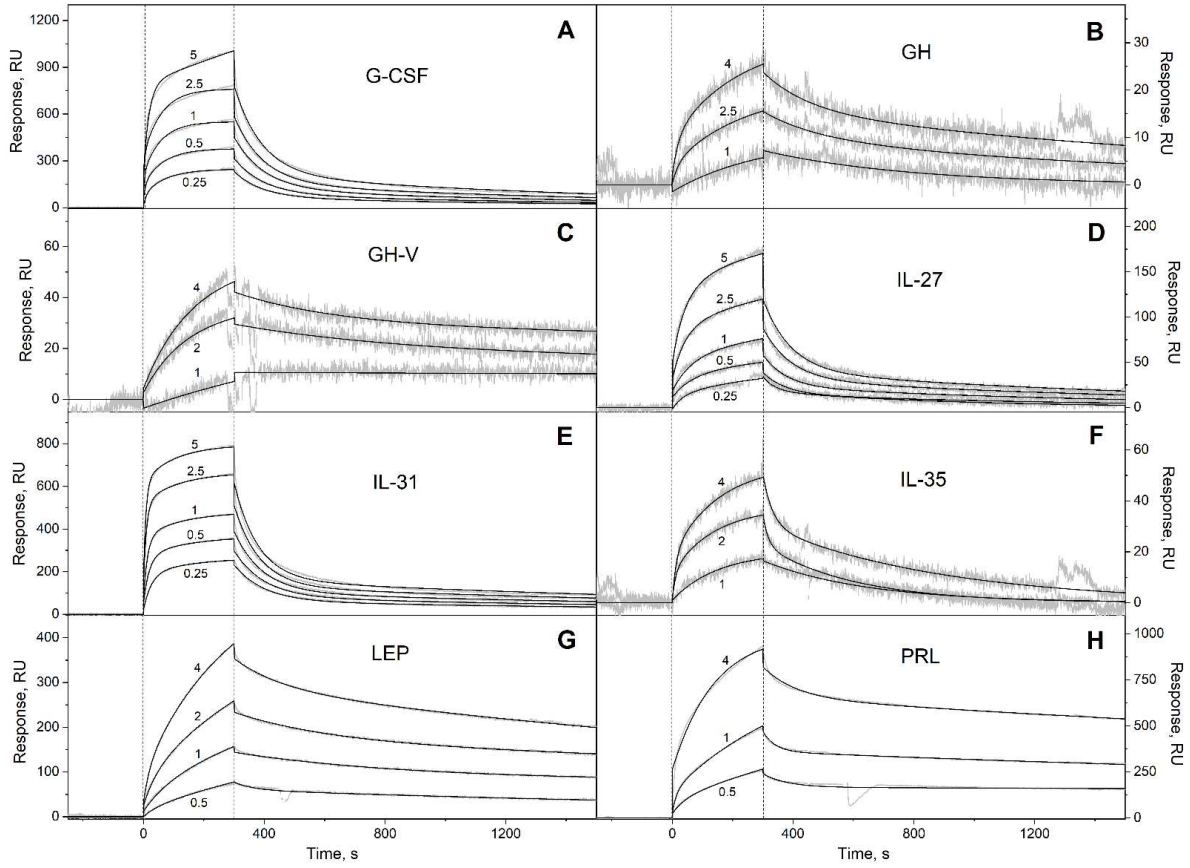


**Figure 3.** SPR spectroscopy data on kinetics of association/dissociation of the complexes of $Ca^{2+}$-loaded S100A6 with the long-chain four-helical cytokines (see Table 3) immobilized on the sensor chip surface by amine coupling, 25°C (10 mM HEPES, 150 mM NaCl, 1 mM $CaCl_2$, 0.05% TWEEN 20, pH 7.4). The experimental curves (*grey*) are described by the *heterogeneous ligand* model (1) (*black curves*) (see Table 3). For other designations, refer to the caption to Figure 1.

Preprints (www.preprints.org) | NOT PEER-REVIEWED | Posted: 28 July 2023 doi:10.20944/preprints202307.2030.v1



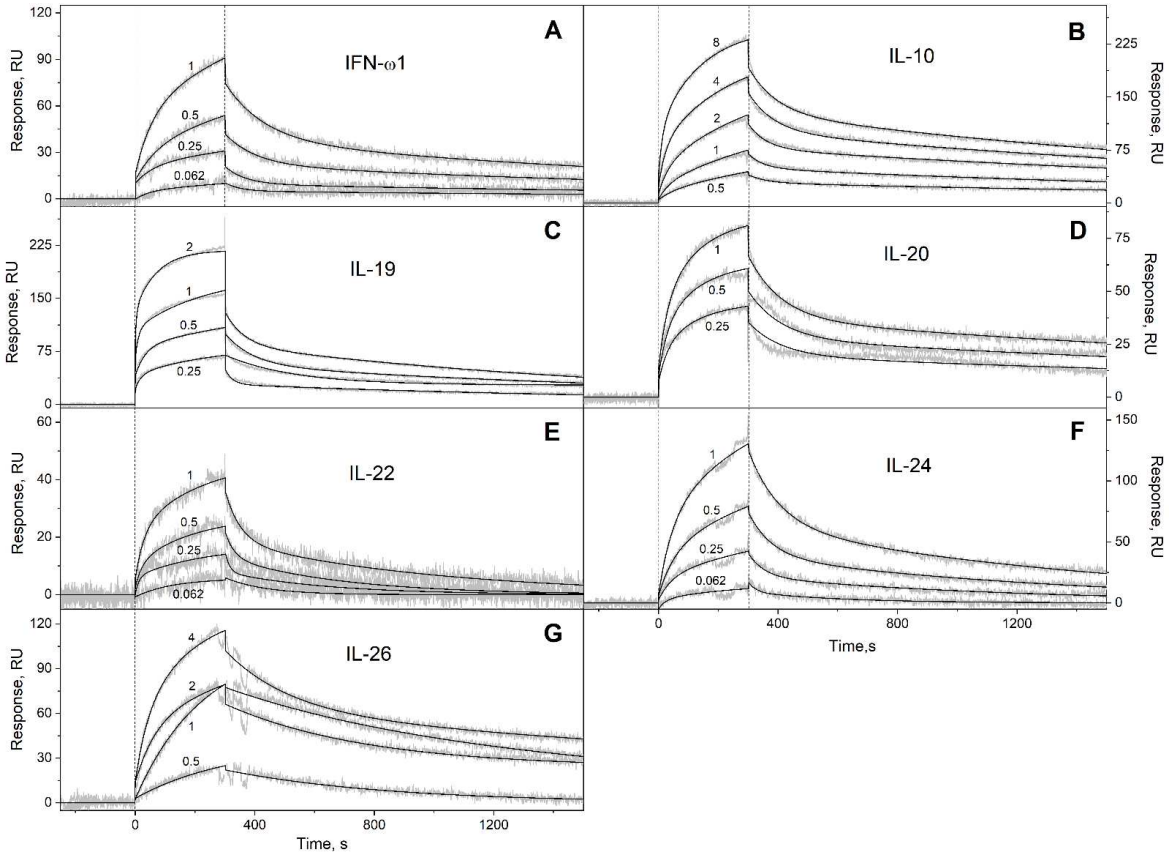


**Figure 4.** SPR spectroscopy data on kinetics of association/dissociation of the complexes of $Ca^{2+}$-bound S100A6 with the interferons/IL-10 four-helical cytokines (see Table 3) immobilized on the sensor chip surface by amine coupling, 25°C (10 mM HEPES, 150 mM NaCl, 1 mM $CaCl_2$, 0.05% TWEEN 20, pH 7.4). The experimental curves (*grey*) are described by the *heterogeneous ligand* model (1) (*black curves*) (see Table 3). For other designations, refer to the caption to Figure 1.

**Table 3.** Parameters of the interactions between $Ca^{2+}$-bound S100A6 and specific four-helical cytokines shown in Table 2 at 25°C, derived from the SPR spectroscopy data (Figures 1–4) using the *heterogeneous ligand* model (1).

| *Cytokine* | $k_{a1}$, $s^{-1}$ | $K_{a1}$, *M* | $k_{a2}$, $s^{-1}$ | $K_{a2}$, *M* |
|---|---|---|---|---|
| *Short-chain cytokines* | | | | |
| Flt3L | $(8.83 \pm 2.54) \times 10^{-4}$ | $(1.22 \pm 0.27) \times 10^{-7}$ | $(8.32 \pm 4.05) \times 10^{-4}$ | $(1.25 \pm 0.46) \times 10^{-7}$ |
| GM-CSF | $(7.92 \pm 4.02) \times 10^{-4}$ | $(2.26 \pm 1.18) \times 10^{-6}$ | $(1.76 \pm 0.49) \times 10^{-2}$ | $(3.63 \pm 1.14) \times 10^{-6}$ |
| IL-2* | $(4.97 \pm 0.78) \times 10^{-3}$ | $(1.20 \pm 0.04) \times 10^{-5}$ | n/a | n/a |
| IL-3 | $(2.71 \pm 0.78) \times 10^{-4}$ | $(6.11 \pm 2.19) \times 10^{-9}$ | $(7.28 \pm 0.65) \times 10^{-3}$ | $(4.02 \pm 2.03) \times 10^{-7}$ |
| IL-5 | $(2.47 \pm 0.45) \times 10^{-4}$ | $(1.16 \pm 0.52) \times 10^{-8}$ | $(5.07 \pm 0.20) \times 10^{-3}$ | $(3.23 \pm 0.73) \times 10^{-8}$ |
| IL-9 | $(5.97 \pm 2.79) \times 10^{-3}$ | $(1.69 \pm 0.90) \times 10^{-7}$ | $(5.85 \pm 2.72) \times 10^{-3}$ | $(2.71 \pm 2.42) \times 10^{-7}$ |

 doi:10.20944/preprints202307.2030.v1



| | | | | |
|---|---|---|---|---|
| IL-13 | $(2.64 \pm 0.98) \times 10^{-4}$ | $(1.97 \pm 1.50) \times 10^{-7}$ | $(1.36 \pm 0.06) \times 10^{-2}$ | $(1.91 \pm 1.07) \times 10^{-6}$ |
| IL-15 | $(1.62 \pm 0.24) \times 10^{-4}$ | $(5.70 \pm 0.46) \times 10^{-8}$ | $(6.29 \pm 0.26) \times 10^{-3}$ | $(2.15 \pm 1.32) \times 10^{-7}$ |
| IL-21 | $(1.88 \pm 1.33) \times 10^{-4}$ | $(4.57 \pm 1.30) \times 10^{-8}$ | $(5.68 \pm 0.34) \times 10^{-3}$ | $(3.87 \pm 0.86) \times 10^{-7}$ |
| SCF | $(2.57 \pm 0.92) \times 10^{-4}$ | $(8.72 \pm 4.95) \times 10^{-9}$ | $(4.51 \pm 1.52) \times 10^{-3}$ | $(1.90 \pm 1.45) \times 10^{-6}$ |
| THPO | $(6.00 \pm 3.29) \times 10^{-5}$ | $(2.89 \pm 1.83) \times 10^{-10}$ | $(4.47 \pm 2.46) \times 10^{-3}$ | $(3.96 \pm 2.65) \times 10^{-9}$ |
| *Long-chain cytokines* | | | | |
| G-CSF | $(7.72 \pm 0.31) \times 10^{-4}$ | $(3.91 \pm 2.06) \times 10^{-9}$ | $(1.04 \pm 0.04) \times 10^{-2}$ | $(1.68 \pm 1.29) \times 10^{-6}$ |
| GH | $(3.73 \pm 2.36) \times 10^{-4}$ | $(3.42 \pm 2.85) \times 10^{-7}$ | $(5.87 \pm 1.16) \times 10^{-3}$ | $(4.16 \pm 2.65) \times 10^{-7}$ |
| GH-V | $(7.92 \pm 3.35) \times 10^{-5}$ | $(4.62 \pm 2.41) \times 10^{-8}$ | $(3.06 \pm 1.27) \times 10^{-3}$ | $(1.78 \pm 0.92) \times 10^{-6}$ |
| IL-27# | $(9.61 \pm 4.18) \times 10^{-4}$ | $(1.16 \pm 0.63) \times 10^{-6}$ | $(1.47 \pm 0.62) \times 10^{-2}$ | $(2.80 \pm 0.85) \times 10^{-6}$ |
| IL-31 | $(4.64 \pm 0.13) \times 10^{-4}$ | $(1.06 \pm 0.96) \times 10^{-7}$ | $(1.11 \pm 0.12) \times 10^{-2}$ | $(2.56 \pm 1.95) \times 10^{-7}$ |
| IL-35# | $(2.59 \pm 0.81) \times 10^{-3}$ | $(2.34 \pm 1.26) \times 10^{-6}$ | $(3.91 \pm 1.55) \times 10^{-2}$ | $(4.65 \pm 2.42) \times 10^{-6}$ |
| LEP | $(3.18 \pm 2.17) \times 10^{-3}$ | $(3.25 \pm 1.92) \times 10^{-7}$ | $(2.87 \pm 1.00) \times 10^{-4}$ | $(3.85 \pm 1.06) \times 10^{-7}$ |
| PRL | $(1.59 \pm 0.23) \times 10^{-4}$ | $(8.40 \pm 0.58) \times 10^{-8}$ | $(1.55 \pm 0.82) \times 10^{-2}$ | $(6.35 \pm 0.96) \times 10^{-7}$ |
| *Interferons/IL-10* | | | | |
| IFN-ω1 | $(4.71 \pm 0.22) \times 10^{-4}$ | $(2.28 \pm 0.64) \times 10^{-7}$ | $(1.29 \pm 0.55) \times 10^{-2}$ | $(1.11 \pm 0.63) \times 10^{-6}$ |
| IL-10 | $(3.98 \pm 0.28) \times 10^{-4}$ | $(3.61 \pm 1.09) \times 10^{-7}$ | $(1.50 \pm 0.37) \times 10^{-2}$ | $(2.13 \pm 0.67) \times 10^{-6}$ |
| IL-19 | $(6.28 \pm 0.86) \times 10^{-4}$ | $(1.47 \pm 1.08) \times 10^{-7}$ | $(2.77 \pm 1.69) \times 10^{-2}$ | $(4.96 \pm 4.04) \times 10^{-7}$ |
| IL-20 | $(3.08 \pm 0.86) \times 10^{-4}$ | $(4.51 \pm 1.12) \times 10^{-8}$ | $(9.14 \pm 2.51) \times 10^{-3}$ | $(3.85 \pm 0.59) \times 10^{-7}$ |

Preprints (www.preprints.org) | NOT PEER-REVIEWED | Posted: 28 July 2023 doi:10.20944/preprints202307.2030.v1



| | | | | |
|---|---|---|---|---|
| IL-22 | $(3.57 \pm 2.56) \times 10^{-3}$ | $(5.93 \pm 0.84) \times 10^{-7}$ | $(3.26 \pm 2.67) \times 10^{-2}$ | $(1.31 \pm 0.49) \times 10^{-6}$ |
| IL-24 | $(5.73 \pm 0.85) \times 10^{-4}$ | $(2.39 \pm 0.94) \times 10^{-7}$ | $(7.79 \pm 1.72) \times 10^{-3}$ | $(6.01 \pm 1.57) \times 10^{-7}$ |
| IL-26 | $(5.98 \pm 2.92) \times 10^{-4}$ | $(2.78 \pm 2.31) \times 10^{-7}$ | $(2.56 \pm 1.39) \times 10^{-3}$ | $(6.00 \pm 2.63) \times 10^{-7}$ |

* single site binding model is used. # heterodimeric cytokines. n/a, not applicable

The S100A6-cytokine complexes easily dissociated upon removal of $Ca^{2+}$ by passage over the SPR chip of 20 mM EDTA solution, pH 8.0 (data no shown), which evidences an importance of the $Ca^{2+}$-induced structural rearrangement within S100A6 molecule for the efficient interaction with the cytokines. Since $Ca^{2+}$ binding induces solvent exposure of S100A6 residues of helices $\alpha$2 and $\alpha$3 and the 'hinge' between them [51], this region is likely involved in the cytokine recognition.

Since equilibrium homodimer dissociation constant for the $Ca^{2+}$-loaded S100A6 does not exceed 0.5 μM [39], our estimates of its affinities to the cytokines (Table 3) mostly correspond to the dimeric state of S100A6. Meanwhile, serum S100A6 concentrations may be as low as 0.2 pM [58] (Table S3), which points out that in serum S100A6 may exist in monomeric form.

Since affinities of S100P monomer to the four-helical cytokines IL-11 and IFN-β exceed those for S100P dimer by 1.4-2.2 orders of magnitude [22,54,59], S100A6 monomerization is likely to improve its affinity to the four-helical cytokines. In this case, the $K_d$ values for some of the S100A6-cytokine interactions (Flt3L, IL-3, IL-5, IL-9, IL-13, IL-15, IL-21, SCF, THPO; G-CSF, GH, GH-V, IL-31, PRL; IL-19, IL-20, IL-26) may reach nanomolar level or less (Figure 5), which is enough for the efficient cytokine binding to S100A6 at its serum concentrations reaching nanomolar level [58,60–62] (Table S3). Moreover, the local levels of extracellular S100A6 in damaged tissues expressing S100A6 should be even higher, further facilitating the S100A6-cytokine interactions.

Preprints (www.preprints.org) | NOT PEER-REVIEWED | Posted: 28 July 2023 doi:10.20944/preprints202307.2030.v1



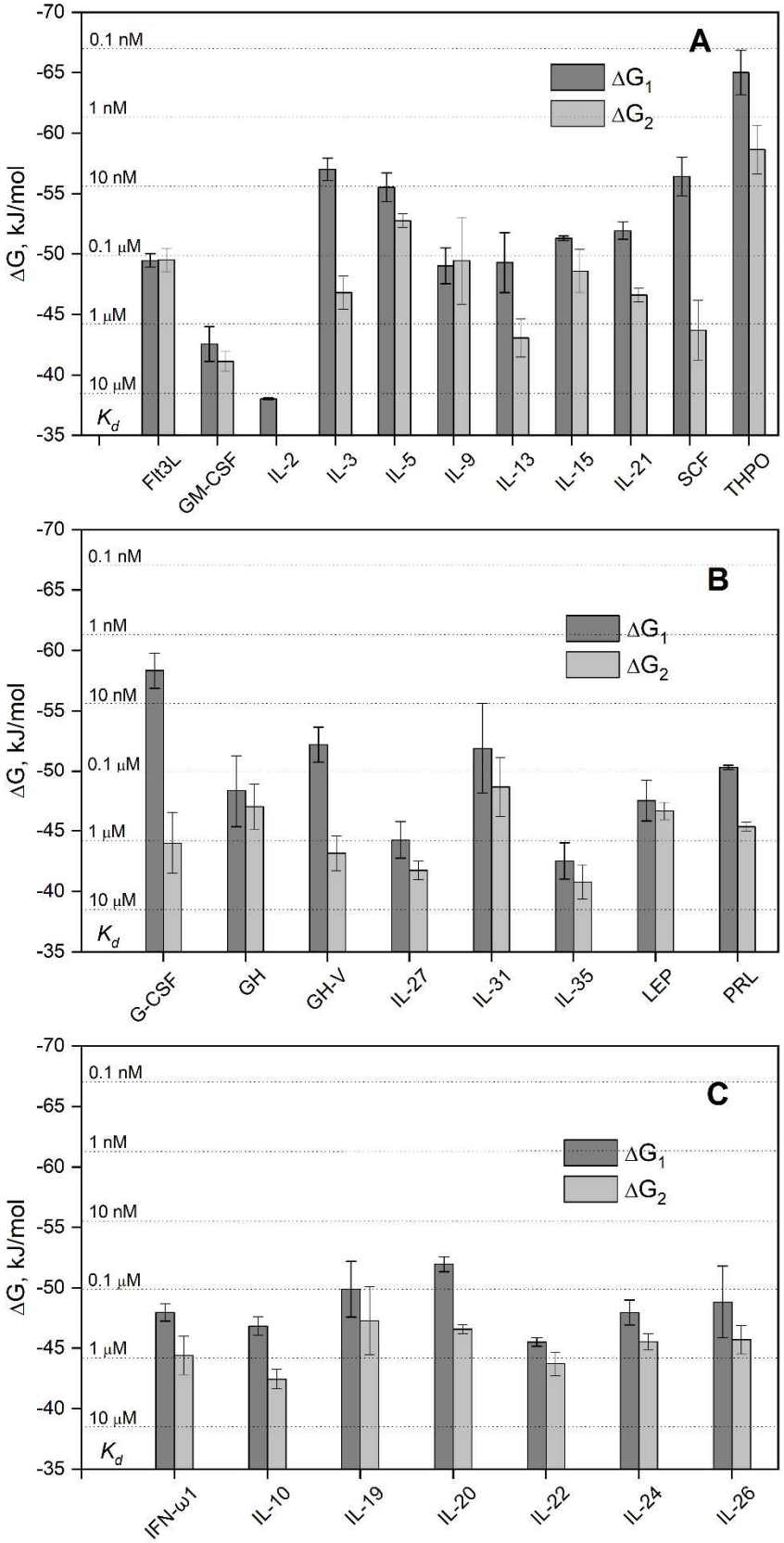


**Figure 5.** The free energy changes upon the binding of $Ca^{2+}$-loaded S100A6 to the four-helical cytokines of short-chain (panel **A**), long-chain (**B**) or interferons/IL-10 (**C**) families at 25°C, estimated from the SPR data shown in Table 3. The scale of $K_d$ values is indicated.

 doi:10.20944/preprints202307.2030.v1



Overall, S100A6 interacts with ca 73% of the four-helical cytokines studied to date (32 of the 44 cytokines, see Tables 1, 3 and S2). The selectivity of S100A6 binding to the cytokines is equivalent to that of S100P [42], except for the interaction with IL-2 and OSM, which are specific only to S100A6 and S100P, respectively. Importantly, the revealed S100A6-cytokine interactions (Table 3) are non-redundant, since the S100A6-specific cytokines are mostly evolutionary distant from each other: the pairwise sequence identities within each of their SCOP families, calculated using Clustal Omega 2.1 (implemented in EMBL-EBI service [11]), ranges from 3% to 44% (the exception is GH – GH-V pair with the pairwise sequence identity of 93%). According to the IntAct [63] and BioGRID [64] databases, so far only S100P protein has been described as a soluble non-receptor extracellular target protein for the following cytokines specific to S100A6 (Table 3): IL-3, IL-5, IL-9, IL-13, IL-21, THPO, IL-22. Except for IL-22, they are short-chain four-helical cytokines with the highest average affinity to S100A6 (Figure 5).

### *3.2. Structural modeling of the S100A6-cytokine complexes*

The docking models of the complexes between $Ca^{2+}$-loaded S100A6 dimer and the S100A6-specific four-helical cytokines shown in Tables 1 and 3 (excluding the heterodimeric IL-27/IL-35) were generated using ClusPro docking server [49] and analyzed as previously described [38,42]. The residues predicted to be involved in the interaction for 5 or more of the 10 docking models are listed in Table S4.

The S100A6 residues predicted to be key for recognition of the four-helical cytokines (for at least half of the cytokines) are I44 (16 cytokines out of 30) of the 'hinge' loop region between helices $\alpha$2 and $\alpha$3, R55 and D59 of helix $\alpha$3 (17 cytokines), and I83 (21 cytokines) and Y84 (18 cytokines) of helix $\alpha$4 (Figure 6A). An analysis of the distribution of the predicted contact residues of S100A6 dimer along its amino acid sequence within the models of its complexes with the four-helical cytokines (Figure 6B) shows that cytokines of the different structural families share the contact surfaces of S100A6, including N- and C-termini, helix $\alpha$1, 'hinge' region, and helices $\alpha$3 and $\alpha$4. These regions of S100A6 dimer form a well-defined cytokine-binding site located between its subunits (Figure 6A), which is remarkably similar to that previously predicted for S100P interaction with the four-helical cytokines [42]. The qualitative difference between the predicted behavior of S100A6 and S100P proteins is the more complete involvement into the cytokine recognition of the helix $\alpha$3 and N-terminal half of the helix $\alpha$4 of S100A6. In this sense, the predicted pattern of the contact residues of S100A6 is more reminiscent of that described for S100 proteins, with frequent involvement in target recognition of helix $\alpha$1, 'hinge', and helices $\alpha$3 and $\alpha$4 [65]. Importantly, only 4 of the 11 residues of S100A6 previously shown to interact with V domain of RAGE using NMR [57] are predicted to interact with some of the cytokines (4 out of 30): R62 (GH-V, IL-11, IFN-$\beta$, IL-20), N63 (IL-11, IFN-$\beta$), K64 (IFN-$\beta$), N69 (IL-11) (Table S4). The RAGE-binding site of S100A6 reported in [66] is even more distinct from the predicted cytokine-specific site. Thus, the latter is notably different from the RAGE-binding site.

Preprints (www.preprints.org) | NOT PEER-REVIEWED | Posted: 28 July 2023 doi:10.20944/preprints202307.2030.v1



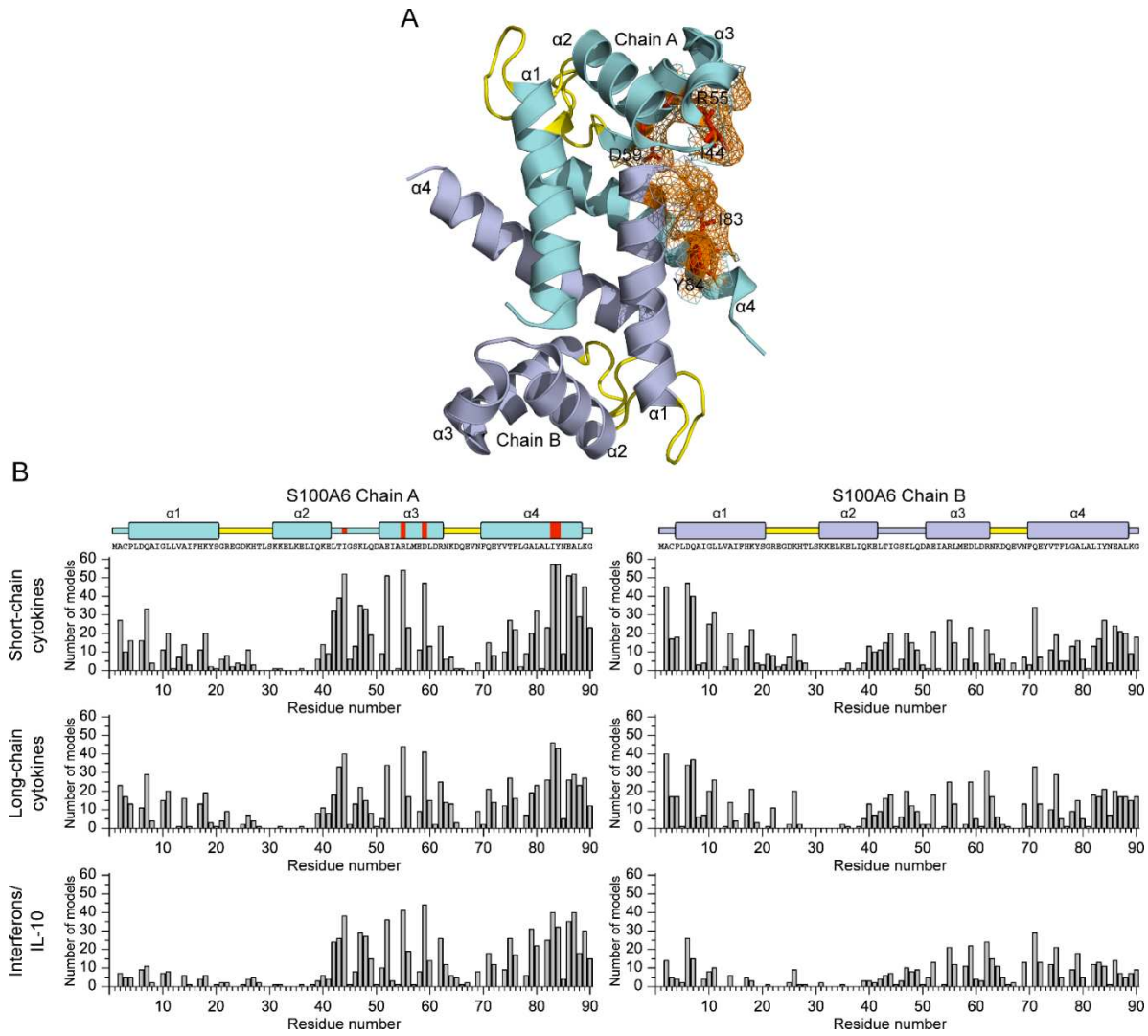


**Figure 6. A**, the cytokine-binding site predicted for the $Ca^{2+}$-loaded S100A6 dimer (PDB entry 1K9K) using ClusPro docking server [49] and the tertiary structures listed in Table S1. The chains A and B are highlighted in cyan and grey, respectively. The α-helices are labeled as α1-α4, and the $Ca^{2+}$-binding loops are yellow-colored. The S100A6 residues predicted to recognize at least 10 out of the 30 four-helical cytokines (I44, E52, R55, D59, I83, Y84, E86, A87 and K89 of chain A, and A2 and D6 of chain B) are marked as an orange mesh surface, whereas the residues predicted to interact with at least half of the cytokines (I44, R55, D59, I83 and Y84) are shown as red balls and sticks. **B**, distributions of the predicted contact residues of S100A6 over its amino acid sequence within the docking models of S100A6 complexes with the four-helical cytokines shown in Table S1 (10 models per each S100A6-cytokine pair). The boundaries of the α-helices α1-α4 are extracted from PDB entry 1K9K; the residues I44, R55, D59, I83, and Y84 of chain A are marked in red.

The molecular docking analysis indicates that the long-chain cytokines preferentially bind $Ca^{2+}$-bound S100A6 dimer by the residues of N-terminus and helices α1 and α3 (Figure 7B). The cytokines of interferons/IL-10 family are predicted to bind S100A6 dimer via the residues of C-terminus and helices α2 and α3 (Figure 7C). Meanwhile, the predicted locations of the contact residues for the short-chain cytokines do not reveal clear regularities (Figure 7A).

Preprints (www.preprints.org) | NOT PEER-REVIEWED | Posted: 28 July 2023 doi:10.20944/preprints202307.2030.v1



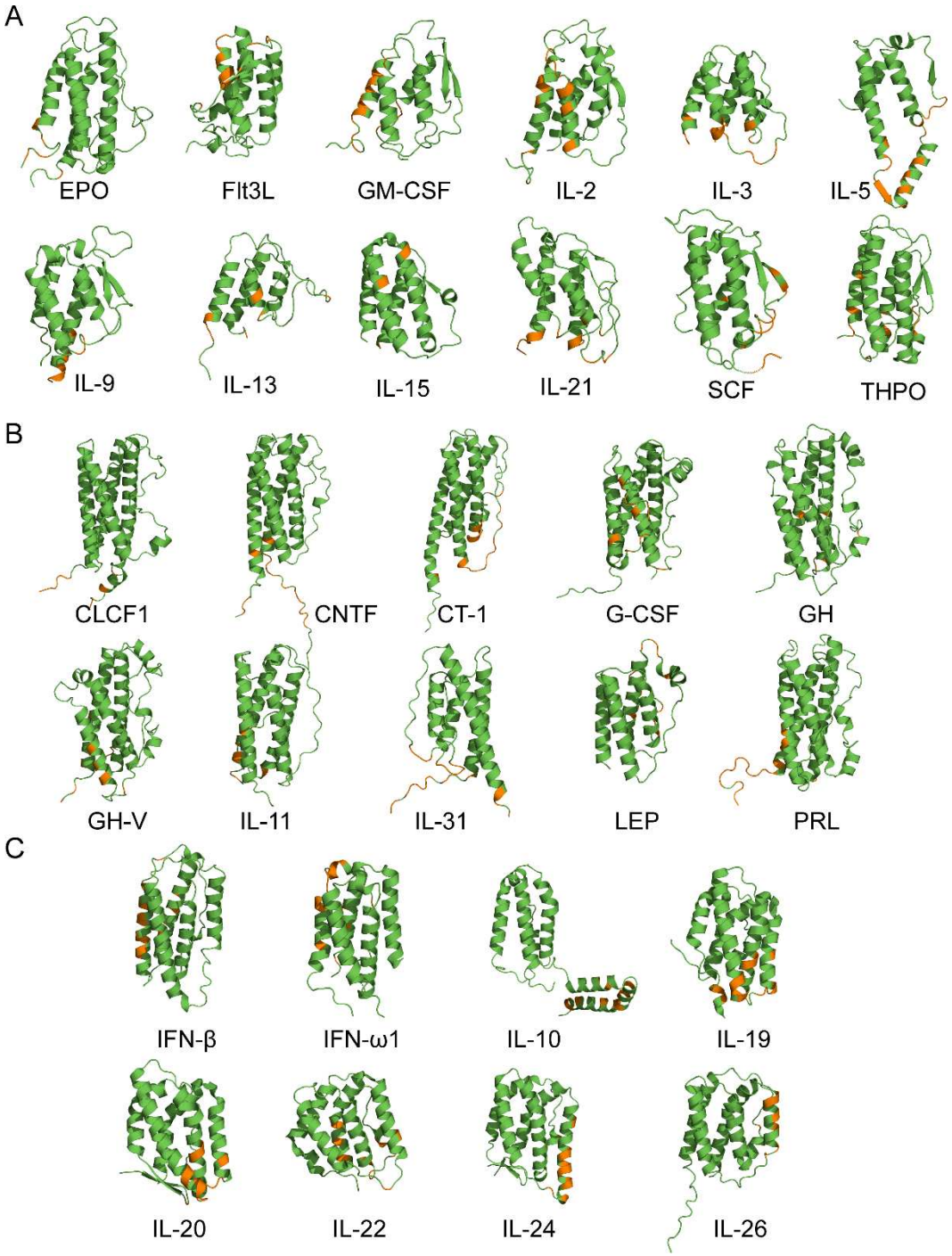


**Figure 7.** The S100A6-binding sites (orange-colored; see Table S4) predicted for the four-helical cytokines of short-chain (panel **A**), long-chain (**B**) and interferons/IL-10 (**C**) families using ClusPro docking server [49] and the tertiary structures listed in Table S1. Only one subunit of IL-5 is shown. N-terminus of each cytokine is located in the lower left corner.

Furthermore, unlike other families of the cytokines, this family tends to interact with only one chain of S100A6 dimer. Therefore, similarly to S100P binding to the four-helical cytokines [42], the putative location of the S100A6-binding site in the cytokines varies depending on structural family of the cytokine and the particular cytokine.

The cytokine residues predicted to interact with S100A6 for some of the short-chain cytokines (GM-CSF, IL-3, IL-13, IL-21, THPO), long-chain cytokines (GH, GH-V, IL-31, PRL) and cytokines of interferons/IL-10 family (IFN-ω1, IL-10, IL-20, IL-22, IL-24) overlap by more than 50% with the

 doi:10.20944/preprints202307.2030.v1



residues similarly predicted for interaction with S100P protein [42]. On the contrary, the putative S100A6-binding sites of specific short-chain cytokines (EPO, IL-5, IL-15), long-chain cytokines (LEP) and cytokines of interferons/IL-10 family (IFN-β, IL-26) do not intersect with the sites predicted for S100P binding [38,42]. Thus, despite the nearly identical selectivity of S100A6 and S100P proteins with regard to binding of the four-helical cytokines and the similar putative locations of their cytokine-binding sites, they could be recognized by the cytokines quite differently.

Since some of the predicted S100A6-binding residues of the specific four-helical cytokines (EPO, GM-CSF, IL-2, IL-3, IL-5, IL-13, IL-15, IL-21, GH, IFN-ω1, IL-20, IL-22 and IL-24) have previously been shown to participate in recognition of their respective receptors (Table S4), S100A6 binding is potentially able to affect the cytokine signaling, as exemplified by the inhibition of IFN-β signaling in MCF-7 cells by S100A1/A4/B/P [22,39,40], suppression of the cytotoxic activity of soluble TNF against Huh-7 cells by S100A12/A13 [37], inhibition of FGF2-induced increase in proliferation of MCF-7/MDA-MB468 cells by S100B [36], and S100A4 stimulation of the amphiregulin-mediated proliferation of embryonic fibroblasts [33].

Of note, the presented structural predictions based on the molecular docking suffer from an inability to take into consideration the structural flexibility inherent to the four-helical cytokines, as evidenced by the experimentally confirmed disorder in IL-15, THPO, G-CSF, LEP, IL-10 and the theoretical predictions described in [42].

### *3.3. Potential physiological significance of the S100A6 interactions with the four-helical cytokines*

To get an insight into possible relative *in vivo* concentrations of S100A6 and the S100A6-specific cytokines (Tables 1 and 3), we collected literature data on their concentrations in physiological fluids under normal and pathological conditions (Tables S3 and S5). Examination of the concentration ranges reported for S100A6 and the S100A6-specific cytokines in the blood serum/plasma (Figure 8) highlights several regularities. First, there is an overlap of the concentration ranges for the both interaction partners, which indicates a possibility of mutual regulation of activity of one of the partners due to an excess of the other partner. The binding of S100A6 could alter the cytokine signaling, as previously shown for IFN-β signaling in MCF-7 cells inhibited by S100A1/A4/B/P [22,39,40], and in other cases [33,36,37]. Alternatively, an excess of the S100A6-specific cytokine over S100A6 protein could affect its interaction with RAGE [56], integrin β1 [25] and/or other receptors. Second, with a few exceptions, there is a trend towards increased cytokine concentrations in pathological conditions, which should promote formation of the S100A6-cytokine complex. The most favorable conditions for that are expected for GH, GH-V, LEP, PRL and IL-26, which demonstrate the highest blood levels, exceeding 1 nM (Figure 8). As mentioned above, although the experimental estimates of the equilibrium dissociation constants (Table 3 and Figure 5), $K_d$, are low enough for efficient S100A6 binding only for THPO, S100A6 monomerization could decrease the $K_d$ values by 1.4-2.2 orders of magnitude, which was earlier shown for S100P interaction with IL-11 and IFN-β [22,54,59]. In this case, many other cytokines could bind S100A6 *in vivo* at concentrations as high as several nM [60] (Table S3).

The binding of S100A6 to the cytokines may also promote their non-canonical secretion, as previously reported for S100A13 binding to IL-1α and FGF1 [34,35] and for CLCF1, which requires CRLF1 binding for efficient secretion [67]. Considering that sharing of interaction partners is inherent to many S100 proteins, including S100A6 and S100P [44,45], the revealed multiple interactions of the four-helical cytokines with S100A6/S100P and other members of S100 family [22,38–42,53,54] could serve as a common mechanism for non-canonical secretion of the cytokines.

Preprints (www.preprints.org) | NOT PEER-REVIEWED | Posted: 28 July 2023 doi:10.20944/preprints202307.2030.v1



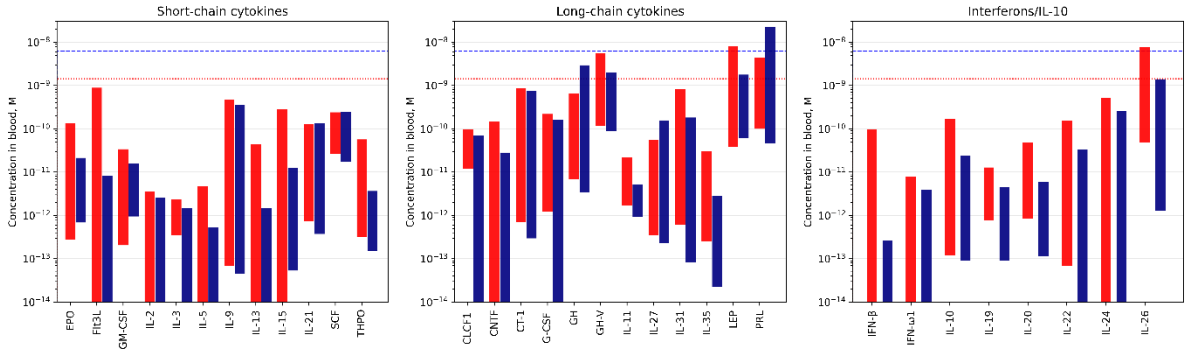


**Figure 8.** The concentration ranges of the S100A6-specific cytokines in the blood serum or plasma under normal (*blue bars*) and pathological (*red bars*) conditions, extracted from the literature data (see Table S6). The blue and red dotted lines correspond to the upper limits of S100A6 serum levels in health and disease, respectively, according to the literature data (see Table S3).

## 4. Conclusions

In this work, we have extended the list of the four-helical cytokines studied with regard to their affinity to the promiscuous S100A6 protein [44,45] from 9 (see references to Table 1) to 44 (see also Table 2) cytokines, covering all structural families of this fold. Only 12 out of the 44 cytokines studied using SPR spectroscopy lack notable specificity to S100A6 (Table S2). The absence of detectable interactions implies that the respective equilibrium dissociation constants, $K_d$, exceed $10^{-4}$ M. Thus, about 73% of the cytokines are specific to $Ca^{2+}$-loaded S100A6 dimer with the $K_d$ values in the range from 0.3 nM to 12 μM (Table 3), which intersects with the $K_d$ estimates for the complexes of $Ca^{2+}$-bound S100A6 with extracellular RAGE fragments from 28 nM to 13 μM [55–57]. The fraction of the cytokines specific to S100A6 may be even higher, given the possibility that S100A6 monomerization promotes its interaction with the cytokines. The similarly high percentage of the four-helical cytokines specific to S100P protein of 71% [42] cannot be attributed to high homology between S100A6 and S100P, since their pairwise sequence identity is only 35%.

The promiscuous binding of S100A6 and S100P to wide range of the four-helical cytokines belonging to all structural families of this fold can be partly explained by the molecular docking analysis, which revealed that both S100 proteins have a nearly identical cytokine-binding site formed by helices α1, α3 and α4, and 'hinge' (Figure 6A, [42]). The involvement of 'hinge' and helix α4 in the cytokine recognition was previously confirmed by S100P mutagenesis [42]. This site overlaps with the RAGE-binding site of S100P, but differs markedly from that for S100A6. Meanwhile, the structural modeling shows that the S100-specific four-helical cytokines lack a conserved S100-binding site (Figure 7, [42]). Instead, the location of the putative S100A6/S100P-binding sites of the cytokines is variable and depends on the particular cytokine. Importantly, the modelling reveals distinct differences in the cytokine regions putatively involved in the recognition of S100A6 or S100P proteins, which explains some differences in their selectivity to the cytokines (limited to recognition of IL-2 and OSM). Nevertheless, similarly to the putative S100P-binding sites of the four-helical cytokines [42], some of their predicted S100A6-specific regions are involved in binding of the corresponding receptors. This fact raises the possibility that the interaction of some cytokines with extracellular S100A6/S100P may interfere with formation of the cytokine-receptor complexes, thereby inhibiting the proper signaling (see, for instance, [22,36,37,39,40]). The same effect is expected for other promiscuous members of S100 family, capable of interaction with multiple common binding partners [44,45]. In this case, the promiscuous S100 proteins are potentially able to serve as universal inhibitors of signaling of the four-helical cytokines. This unique feature of the S100 family could be used for reduction of severity of the disorders associated with excessive release of the cytokines, including cytokine storm. Another possibility is the cytokine binding-induced modulation of extracellular activity of the promiscuous S100 proteins in response to the pathological conditions accompanied by

elevated levels of some four-helical cytokines. Finally, the binding of intracellular S100 proteins could facilitate the non-canonical secretion of certain cytokines [34,35,67].

**Supplementary Materials:** The following supporting information can be downloaded at: www.mdpi.com/xxx/s1, Table S1: The PDB entries or AlphaFold2 predictions used for structural modelling of the complexes of Ca2+-loaded human S100A6 dimer (chains A, B of PDB entry 1K9K) with the four-helical cytokines using ClusPro docking server; Table S2: The samples of the four-helical cytokines lacking specificity to S100A6, as evidenced by SPR experiments using cytokine as a ligand; Table S3: Serum levels of S100A6 under normal and pathological conditions, according to the literature data; Table S4: The contact residues for the S100A6-cytokine complexes predicted using ClusPro docking server (numbering is according to the PDB entries); Table S5: The literature data on concentrations of the S100A6-specific four-helical cytokines in the physiological fluids under normal and pathological conditions; Table S6: The concentration ranges of the S100A6-specific cytokines in the physiological fluids under normal and pathological conditions, extracted from the literature data collected in Table S5. .

**Author Contributions:** Conceptualization, S.E.P.; validation, A.S.K., E.I.D., V.A.R., V.N.U., E.A.P., S.E.P.; formal analysis, A.S.K., E.I.D., V.A.R., S.E.P.; investigation, A.S.K., E.I.D., V.A.R., A.S.S., M.E.P., E.A.L.; data curation, A.S.K., E.I.D., V.A.R., S.E.P.; writing—original draft preparation, A.S.K., E.I.D., V.A.R., S.E.P.; writing—review and editing, A.S.K., E.I.D., V.A.R., V.N.U., E.A.P., S.E.P.; supervision, E.A.P., S.E.P.; project administration, S.E.P.; funding acquisition, S.E.P. All authors have read and agreed to the published version of the manuscript.

**Funding:** This research was funded by Russian Science Foundation, grant number 19-14-00289-П to S.E.P.

**Institutional Review Board Statement:** Not applicable.

**Informed Consent Statement:** Not applicable.

**Data Availability Statement:** The data present in the current study are available from the corresponding authors on reasonable request.

**Conflicts of Interest:** The authors declare no conflict of interest. The funders had no role in the design of the study; in the collection, analyses, or interpretation of data; in the writing of the manuscript; or in the decision to publish the results.

### Abbreviations

CHO, Chinese hamster ovary cells; CLCF1, cardiotrophin-like cytokine factor 1; CNTF, ciliary neurotrophic factor; CT-1, cardiotrophin-1; EDTA, ethylenediaminetetraacetic acid; EPO, erythropoietin; FGF, fibroblast growth factor; ER, endoplasmic reticulum; Flt3L, Fms-related tyrosine kinase 3 ligand; G-CSF, granulocyte colony-stimulating factor; GH, growth hormone; GH-V, growth hormone variant; GM-CSF, granulocyte-macrophage colony-stimulating factor; HEK293, Human embryonic kidney 293 cells; HEPES, 4-(2-hydroxyethyl)piperazine-1-ethanesulfonic acid; IFN, interferon; IL, interleukin; LEP, leptin; LIF, leukemia inhibitory factor; M-CSF, macrophage colony-stimulating factor 1; NMR, nuclear magnetic resonance; OSM, oncostatin-M; PDB, Protein Data Bank [50]; PL, chorionic somatomammotropin hormone 1; PRL, prolactin; RAGE, receptor for advanced glycation end products; RU, resonance unit; SCF, stem cell factor, soluble form; SCOP, Structural Classification of Proteins [43]; SPR, surface plasmon resonance; THPO, thrombopoietin; TNF, Tumor necrosis factor; TSLP, thymic stromal lymphopoietin.

## References

1. Donato, R.; Cannon, B.R.; Sorci, G.; Riuzzi, F.; Hsu, K.; Weber, D.J.; Geczy, C.L. Functions of S100 Proteins. *Curr Mol Med* **2013**, *13*, 24-57, doi:10.2174/156652413804486214.
2. Sreejit, G.; Flynn, M.C.; Patil, M.; Krishnamurthy, P.; Murphy, A.J.; Nagareddy, P.R. S100 family proteins in inflammation and beyond. *Adv Clin Chem* **2020**, *98*, 173-231, doi:10.1016/bs.acc.2020.02.006.
3. Singh, P.; Ali, S.A. Multifunctional Role of S100 Protein Family in the Immune System: An Update. *Cells* **2022**, *11*, doi:10.3390/cells11152274.
4. Zimmer, D.B.; Eubanks, J.O.; Ramakrishnan, D.; Criscitiello, M.F. Evolution of the S100 family of calcium sensor proteins. *Cell Calcium* **2013**, *53*, 170-179, doi:10.1016/j.ceca.2012.11.006.
5. Sigrist, C.J.; de Castro, E.; Cerutti, L.; Cuche, B.A.; Hulo, N.; Bridge, A.; Bougueleret, L.; Xenarios, I. New and continuing developments at PROSITE. *Nucleic Acids Res* **2013**, *41*, D344-347, doi:10.1093/nar/gks1067.
6. Nockolds, C.E.; Kretsinger, R.H.; Coffee, C.J.; Bradshaw, R.A. Structure of a calcium-binding carp myogen. *Proc.Natl.Acad.Sci.U.S.A* **1972**, *69*, 581-584, doi:10.1073/pnas.69.3.581.
7. Gifford, J.L.; Walsh, M.P.; Vogel, H.J. Structures and metal-ion-binding properties of the Ca2+-binding helix-loop-helix EF-hand motifs. *Biochem J* **2007**, *405*, 199-221, doi:10.1042/BJ20070255.

8. Fritz, G.; Heizmann, C.W. 3D Structures of the Calcium and Zinc Binding S100 Proteins. In *Handbook of Metalloproteins*, John Wiley & Sons, L., Ed. 2004; doi:10.1002/0470028637.met046.
9. Gilston, B.A.; Skaar, E.P.; Chazin, W.J. Binding of transition metals to S100 proteins. *Sci China Life Sci* **2016**, *59*, 792-801, doi:10.1007/s11427-016-5088-4.
10. Streicher, W.W.; Lopez, M.M.; Makhatadze, G.I. Modulation of quaternary structure of S100 proteins by calcium ions. *Biophys Chem* **2010**, *151*, 181-186, doi:10.1016/j.bpc.2010.06.003.
11. Madeira, F.; Park, Y.M.; Lee, J.; Buso, N.; Gur, T.; Madhusoodanan, N.; Basutkar, P.; Tivey, A.R.N.; Potter, S.C.; Finn, R.D., et al. The EMBL-EBI search and sequence analysis tools APIs in 2019. *Nucleic acids research* **2019**, *47*, W636-W641, doi:10.1093/nar/gkz268.
12. Bresnick, A.R.; Weber, D.J.; Zimmer, D.B. S100 proteins in cancer. *Nat Rev Cancer* **2015**, *15*, 96-109, doi:10.1038/nrc3893.
13. Cristóvão, J.S.; Gomes, C.M. S100 Proteins in Alzheimer's Disease. *Front Neurosci-Switz* **2019**, *13*, 463, doi:10.3389/Fnins.2019.00463.
14. Holzinger, D.; Tenbrock, K.; Roth, J. Alarmins of the S100-Family in Juvenile Autoimmune and Auto-Inflammatory Diseases. *Front Immunol* **2019**, *10*, 182-182, doi:10.3389/fimmu.2019.00182.
15. Sattar, Z.; Lora, A.; Jundi, B.; Railwah, C.; Geraghty, P. The S100 Protein Family as Players and Therapeutic Targets in Pulmonary Diseases. *Pulm Med* **2021**, *2021*, 5488591, doi:10.1155/2021/5488591.
16. Gonzalez, L.L.; Garrie, K.; Turner, M.D. Role of S100 proteins in health and disease. *Biochim Biophys Acta Mol Cell Res* **2020**, *1867*, 118677, doi:10.1016/j.bbamcr.2020.118677.
17. Allgower, C.; Kretz, A.L.; von Karstedt, S.; Wittau, M.; Henne-Bruns, D.; Lemke, J. Friend or Foe: S100 Proteins in Cancer. *Cancers (Basel)* **2020**, *12*, doi:10.3390/cancers12082037.
18. Bresnick, A.R. S100 proteins as therapeutic targets. *Biophys Rev* **2018**, *10*, 1617-1629, doi:10.1007/s12551-018-0471-y.
19. Engelkamp, D.; Schafer, B.W.; Mattei, M.G.; Erne, P.; Heizmann, C.W. Six S100 genes are clustered on human chromosome 1q21: identification of two genes coding for the two previously unreported calcium-binding proteins S100D and S100E. *Proc Natl Acad Sci U S A* **1993**, *90*, 6547-6551, doi:10.1073/pnas.90.14.6547.
20. Schafer, B.W.; Wicki, R.; Engelkamp, D.; Mattei, M.G.; Heizmann, C.W. Isolation of a YAC clone covering a cluster of nine S100 genes on human chromosome 1q21: rationale for a new nomenclature of the S100 calcium-binding protein family. *Genomics* **1995**, *25*, 638-643.
21. Marenholz, I.; Lovering, R.C.; Heizmann, C.W. An update of the S100 nomenclature. *Biochim Biophys Acta* **2006**, *1763*, 1282-1283, doi:10.1016/j.bbamcr.2006.07.013.
22. Kazakov, A.S.; Mayorov, S.A.; Deryusheva, E.I.; Avkhacheva, N.V.; Denessiouk, K.A.; Denesyuk, A.I.; Rastrygina, V.A.; Permyakov, E.A.; Permyakov, S.E. Highly specific interaction of monomeric S100P protein with interferon beta. *Int J Biol Macromol* **2020**, *143*, 633-639, doi:10.1016/j.ijbiomac.2019.12.039.
23. Hsieh, H.L.; Schafer, B.W.; Cox, J.A.; Heizmann, C.W. S100A13 and S100A6 exhibit distinct translocation pathways in endothelial cells. *J Cell Sci* **2002**, *115*, 3149-3158, doi:10.1242/jcs.115.15.3149.
24. Jurewicz, E.; Wyroba, E.; Filipek, A. Tubulin-dependent secretion of S100A6 and cellular signaling pathways activated by S100A6-integrin beta1 interaction. *Cell Signal* **2018**, *42*, 21-29, doi:10.1016/j.cellsig.2017.10.004.
25. Jurewicz, E.; Góral, A.; Filipek, A. S100A6 is secreted from Wharton's jelly mesenchymal stem cells and interacts with integrin β1. *The International Journal of Biochemistry & Cell Biology* **2014**, *55*, 298-303, doi:10.1016/j.biocel.2014.09.015.
26. Rumpret, M.; von Richthofen, H.J.; van der Linden, M.; Westerlaken, G.H.A.; Talavera Ormeno, C.; Low, T.Y.; Ovaa, H.; Meyaard, L. Recognition of S100 proteins by Signal Inhibitory Receptor on Leukocytes-1 negatively regulates human neutrophils. *Eur J Immunol* **2021**, *51*, 2210-2217, doi:10.1002/eji.202149278.
27. Moller, A.; Jauch-Speer, S.L.; Gandhi, S.; Vogl, T.; Roth, J.; Fehler, O. The roles of toll-like receptor 4, CD33, CD68, CD69, or CD147/EMMPRIN for monocyte activation by the DAMP S100A8/S100A9. *Front Immunol* **2023**, *14*, 1110185, doi:10.3389/fimmu.2023.1110185.
28. Ruma, I.M.; Putranto, E.W.; Kondo, E.; Murata, H.; Watanabe, M.; Huang, P.; Kinoshita, R.; Futami, J.; Inoue, Y.; Yamauchi, A., et al. MCAM, as a novel receptor for S100A8/A9, mediates progression of malignant melanoma through prominent activation of NF-κB and ROS formation upon ligand binding. *Clin Exp Metastasis* **2016**, *33*, 609-627, doi:10.1007/s10585-016-9801-2.
29. Sakaguchi, M.; Yamamoto, M.; Miyai, M.; Maeda, T.; Hiruma, J.; Murata, H.; Kinoshita, R.; Winarsa Ruma, I.M.; Putranto, E.W.; Inoue, Y., et al. Identification of an S100A8 Receptor Neuroplastin-beta and its Heterodimer Formation with EMMPRIN. *J Invest Dermatol* **2016**, *136*, 2240-2250, doi:10.1016/j.jid.2016.06.617.
30. Tomonobu, N.; Kinoshita, R.; Sakaguchi, M. S100 Soil Sensor Receptors and Molecular Targeting Therapy Against Them in Cancer Metastasis. *Transl Oncol* **2020**, *13*, 100753, doi:10.1016/j.tranon.2020.100753.

31. Pankratova, S.; Klingelhofer, J.; Dmytriyeva, O.; Owczarek, S.; Renziehausen, A.; Syed, N.; Porter, A.E.; Dexter, D.T.; Kiryushko, D. The S100A4 Protein Signals through the ErbB4 Receptor to Promote Neuronal Survival. *Theranostics* **2018**, *8*, 3977-3990, doi:10.7150/thno.22274.
32. Warner-Schmidt, J.L.; Flajolet, M.; Maller, A.; Chen, E.Y.; Qi, H.; Svenningsson, P.; Greengard, P. Role of p11 in cellular and behavioral effects of 5-HT4 receptor stimulation. *J Neurosci* **2009**, *29*, 1937-1946, doi:10.1523/JNEUROSCI.5343-08.2009.
33. Klingelhofer, J.; Moller, H.D.; Sumer, E.U.; Berg, C.H.; Poulsen, M.; Kiryushko, D.; Soroka, V.; Ambartsumian, N.; Grigorian, M.; Lukanidin, E.M. Epidermal growth factor receptor ligands as new extracellular targets for the metastasis-promoting S100A4 protein. *Febs J* **2009**, *276*, 5936-5948, doi:10.1111/j.1742-4658.2009.07274.x.
34. Mohan, S.K.; Yu, C. The IL1alpha-S100A13 heterotetrameric complex structure: a component in the non-classical pathway for interleukin 1alpha secretion. *J Biol Chem* **2011**, *286*, 14608-14617, doi:10.1074/jbc.M110.201954.
35. Carreira, C.M.; LaVallee, T.M.; Tarantini, F.; Jackson, A.; Lathrop, J.T.; Hampton, B.; Burgess, W.H.; Maciag, T. S100A13 is involved in the regulation of fibroblast growth factor-1 and p40 synaptotagmin-1 release in vitro. *Journal of Biological Chemistry* **1998**, *273*, 22224-22231, doi:10.1074/jbc.273.35.22224.
36. Gupta, A.A.; Chou, R.H.; Li, H.C.; Yang, L.W.; Yu, C. Structural insights into the interaction of human S100B and basic fibroblast growth factor (FGF2): Effects on FGFR1 receptor signaling. *Bba-Proteins Proteom* **2013**, *1834*, 2606-2619, doi:10.1016/j.bbapap.2013.09.012.
37. Kazakov, A.S.; Zemskova, M.Y.; Rystsov, G.K.; Vologzhannikova, A.A.; Deryusheva, E.I.; Rastrygina, V.A.; Sokolov, A.S.; Permyakova, M.E.; Litus, E.A.; Uversky, V.N., et al. Specific S100 Proteins Bind Tumor Necrosis Factor and Inhibit Its Activity. *Int J Mol Sci* **2022**, *23*, doi:10.3390/ijms232415956.
38. Kazakov, A.S.; Deryusheva, E.I.; Sokolov, A.S.; Permyakova, M.E.; Litus, E.A.; Rastrygina, V.A.; Uversky, V.N.; Permyakov, E.A.; Permyakov, S.E. Erythropoietin Interacts with Specific S100 Proteins. *Biomolecules* **2022**, *12*, doi:10.3390/biom12010120.
39. Kazakov, A.S.; Sofin, A.D.; Avkhacheva, N.V.; Denesyuk, A.I.; Deryusheva, E.I.; Rastrygina, V.A.; Sokolov, A.S.; Permyakova, M.E.; Litus, E.A.; Uversky, V.N., et al. Interferon Beta Activity Is Modulated via Binding of Specific S100 Proteins. *International journal of molecular sciences* **2020**, *21*, doi:10.3390/ijms21249473.
40. Kazakov, A.S.; Sofin, A.D.; Avkhacheva, N.V.; Deryusheva, E.I.; Rastrygina, V.A.; Permyakova, M.E.; Uversky, V.N.; Permyakov, E.A.; Permyakov, S.E. Interferon-β Activity Is Affected by S100B Protein. *International journal of molecular sciences* **2022**, *23*, doi:10.3390/ijms23041997.
41. Kazakov, A.S.; Sokolov, A.S.; Permyakova, M.E.; Litus, E.A.; Uversky, V.N.; Permyakov, E.A.; Permyakov, S.E. Specific cytokines of interleukin-6 family interact with S100 proteins. *Cell Calcium* **2022**, *101*, 102520, doi:10.1016/j.ceca.2021.102520.
42. Kazakov, A.S.; Deryusheva, E.I.; Permyakova, M.E.; Sokolov, A.S.; Rastrygina, V.A.; Uversky, V.N.; Permyakov, E.A.; Permyakov, S.E. Calcium-Bound S100P Protein Is a Promiscuous Binding Partner of the Four-Helical Cytokines. *Int J Mol Sci* **2022**, *23*, doi:10.3390/ijms231912000.
43. Andreeva, A.; Kulesha, E.; Gough, J.; Murzin, A.G. The SCOP database in 2020: expanded classification of representative family and superfamily domains of known protein structures. *Nucleic acids research* **2020**, *48*, D376-D382, doi:10.1093/nar/gkz1064.
44. Simon, M.A.; Ecsedi, P.; Kovacs, G.M.; Poti, A.L.; Remenyi, A.; Kardos, J.; Gogl, G.; Nyitray, L. High-throughput competitive fluorescence polarization assay reveals functional redundancy in the S100 protein family. *The FEBS journal* **2020**, *287*, 2834-2846, doi:10.1111/febs.15175.
45. Simon, M.A.; Bartus, É.; Mag, B.; Boros, E.; Roszjár, L.; Gógl, G.; Travé, G.; Martinek, T.A.; Nyitray, L. Promiscuity mapping of the S100 protein family using a high-throughput holdup assay. *Sci Rep* **2022**, *12*, 5904, doi:10.1038/s41598-022-09574-2.
46. Lesniak, W.; Filipek, A. S100A6 Protein-Expression and Function in Norm and Pathology. *Int J Mol Sci* **2023**, *24*, doi:10.3390/ijms24021341.
47. Pace, C.N.; Vajdos, F.; Fee, L.; Grimsley, G.; Gray, T. How to measure and predict the molar absorption coefficient of a protein. *Protein Sci.* **1995**, *4*, 2411-2423, doi:10.1002/pro.5560041120.
48. Brocker, C.; Thompson, D.; Matsumoto, A.; Nebert, D.W.; Vasiliou, V. Evolutionary divergence and functions of the human interleukin (IL) gene family. *Hum Genomics* **2010**, *5*, 30-55, doi:10.1186/1479-7364-5-1-30.
49. Desta, I.T.; Porter, K.A.; Xia, B.; Kozakov, D.; Vajda, S. Performance and Its Limits in Rigid Body Protein-Protein Docking. *Structure* **2020**, *28*, 1071-1081 e1073, doi:10.1016/j.str.2020.06.006.
50. Berman, H.M.; Westbrook, J.; Feng, Z.; Gilliland, G.; Bhat, T.N.; Weissig, H.; Shindyalov, I.N.; Bourne, P.E. The Protein Data Bank. *Nucleic Acids Res.* **2000**, *28*, 235-242, doi:10.1093/nar/28.1.235.
51. Otterbein, L.R.; Kordowska, J.; Witte-Hoffmann, C.; Wang, C.L.; Dominguez, R. Crystal structures of S100A6 in the Ca(2+)-free and Ca(2+)-bound states: the calcium sensor mechanism of S100 proteins revealed at atomic resolution. *Structure* **2002**, *10*, 557-567, doi:10.1016/s0969-2126(02)00740-2.

52. Jumper, J.; Evans, R.; Pritzel, A.; Green, T.; Figurnov, M.; Ronneberger, O.; Tunyasuvunakool, K.; Bates, R.; Zidek, A.; Potapenko, A., et al. Highly accurate protein structure prediction with AlphaFold. *Nature* **2021**, *596*, 583-589, doi:10.1038/s41586-021-03819-2.
53. Kazakov, A.S.; Sokolov, A.S.; Vologzhannikova, A.A.; Permyakova, M.E.; Khorn, P.A.; Ismailov, R.G.; Denessiouk, K.A.; Denesyuk, A.I.; Rastrygina, V.A.; Baksheeva, V.E., et al. Interleukin-11 binds specific EF-hand proteins via their conserved structural motifs. *J Biomol Struct Dyn* **2017**, *35*, 78-91, doi:10.1080/07391102.2015.1132392.
54. Kazakov, A.S.; Sokolov, A.S.; Rastrygina, V.A.; Solovyev, V.V.; Ismailov, R.G.; Mikhailov, R.V.; Ulitin, A.B.; Yakovenko, A.R.; Mirzabekov, T.A.; Permyakov, E.A., et al. High-affinity interaction between interleukin-11 and S100P protein. *Biochem Biophys Res Commun* **2015**, *468*, 733-738, doi:10.1016/j.bbrc.2015.11.024.
55. Leclerc, E. Measuring binding of S100 proteins to RAGE by surface plasmon resonance. *Methods Mol Biol* **2013**, *963*, 201-213, doi:10.1007/978-1-62703-230-8_13.
56. Leclerc, E.; Fritz, G.; Weibel, M.; Heizmann, C.W.; Galichet, A. S100B and S100A6 differentially modulate cell survival by interacting with distinct RAGE (receptor for advanced glycation end products) immunoglobulin domains. *J Biol Chem* **2007**, *282*, 31317-31331, doi:10.1074/jbc.M703951200.
57. Mohan, S.K.; Gupta, A.A.; Yu, C. Interaction of the S100A6 mutant (C3S) with the V domain of the receptor for advanced glycation end products (RAGE). *Biochem Biophys Res Commun* **2013**, *434*, 328-333, doi:10.1016/j.bbrc.2013.03.049.
58. Loosen, S.H.; Benz, F.; Niedeggen, J.; Schmeding, M.; Schuller, F.; Koch, A.; Vucur, M.; Tacke, F.; Trautwein, C.; Roderburg, C., et al. Serum levels of S100A6 are unaltered in patients with resectable cholangiocarcinoma. *Clin Transl Med* **2016**, *5*, 39, doi:10.1186/s40169-016-0120-7.
59. Permyakov, S.E.; Denesyuk, A.I.; Denessiouk, K.A.; Permyakova, M.E.; Kazakov, A.S.; Ismailov, R.G.; Rastrygina, V.A.; Sokolov, A.S.; Permyakov, E.A. Monomeric state of S100P protein: Experimental and molecular dynamics study. *Cell Calcium* **2019**, *80*, 152-159, doi:10.1016/j.ceca.2019.04.008.
60. Guzel, C.; van den Berg, C.B.; Duvekot, J.J.; Stingl, C.; van den Bosch, T.P.P.; van der Weiden, M.; Steegers, E.A.P.; Steegers-Theunissen, R.P.M.; Luider, T.M. Quantification of Calcyclin and Heat Shock Protein 90 in Sera from Women with and without Preeclampsia by Mass Spectrometry. *Proteomics Clin Appl* **2019**, *13*, e1800181, doi:10.1002/prca.201800181.
61. Wang, T.; Liang, Y.; Thakur, A.; Zhang, S.; Yang, T.; Chen, T.; Gao, L.; Chen, M.; Ren, H. Diagnostic significance of S100A2 and S100A6 levels in sera of patients with non-small cell lung cancer. *Tumour Biol* **2016**, *37*, 2299-2304, doi:10.1007/s13277-015-4057-z.
62. Cai, X.Y.; Lu, L.; Wang, Y.N.; Jin, C.; Zhang, R.Y.; Zhang, Q.; Chen, Q.J.; Shen, W.F. Association of increased S100B, S100A6 and S100P in serum levels with acute coronary syndrome and also with the severity of myocardial infarction in cardiac tissue of rat models with ischemia-reperfusion injury. *Atherosclerosis* **2011**, *217*, 536-542, doi:10.1016/j.atherosclerosis.2011.05.023.
63. Orchard, S.; Ammari, M.; Aranda, B.; Breuza, L.; Briganti, L.; Broackes-Carter, F.; Campbell, N.H.; Chavali, G.; Chen, C.; del-Toro, N., et al. The MIntAct project--IntAct as a common curation platform for 11 molecular interaction databases. *Nucleic Acids Res* **2014**, *42*, D358-363, doi:10.1093/nar/gkt1115.
64. Oughtred, R.; Rust, J.; Chang, C.; Breitkreutz, B.J.; Stark, C.; Willems, A.; Boucher, L.; Leung, G.; Kolas, N.; Zhang, F., et al. The BioGRID database: A comprehensive biomedical resource of curated protein, genetic, and chemical interactions. *Protein Sci* **2021**, *30*, 187-200, doi:10.1002/pro.3978.
65. Permyakov, S.E.; Ismailov, R.G.; Xue, B.; Denesyuk, A.I.; Uversky, V.N.; Permyakov, E.A. Intrinsic disorder in S100 proteins. *Mol Biosyst* **2011**, *7*, 2164-2180, doi:10.1039/c0mb00305k.
66. Yatime, L.; Betzer, C.; Jensen, R.K.; Mortensen, S.; Jensen, P.H.; Andersen, G.R. The Structure of the RAGE:S100A6 Complex Reveals a Unique Mode of Homodimerization for S100 Proteins. *Structure* **2016**, *24*, 2043-2052, doi:10.1016/j.str.2016.09.011.
67. Rousseau, F.; Gauchat, J.F.; McLeod, J.G.; Chevalier, S.; Guillet, C.; Guilhot, F.; Cognet, I.; Froger, J.; Hahn, A.F.; Knappskog, P.M., et al. Inactivation of cardiotrophin-like cytokine, a second ligand for ciliary neurotrophic factor receptor, leads to cold-induced sweating syndrome in a patient. *Proceedings of the National Academy of Sciences of the United States of America* **2006**, *103*, 10068-10073, doi:10.1073/pnas.0509598103.